第 33 卷 第 7 期　　焊　接　学　报　　Vol. 33　No. 7
2012 年 7 月　　TRANSACTIONS OF THE CHINA WELDING INSTITUTION　　July　2012

Ti/Al 异种合金电弧熔钎焊接头温度场与界面微观组织

吕世雄[1]，　敬小军[1,2]，　黄永宪[1]，　王远荣[2]，　李蜀非[2]，　徐永强[1]
（1. 哈尔滨工业大学 先进焊接与连接国家重点实验室，哈尔滨　150001；
2. 成都四威高科技产业园有限公司，成都　611731）

摘　要：采用交流 TIG 焊电弧与 AlSi12 焊丝实现了 TC4 钛合金与 LF6 铝合金熔钎焊连接，通过有限元软件分析接头温度场，并利用扫描电镜观察接头钎焊界面的微观组织特征. 结果表明，接头温度分布极不均匀，钛侧梯度大高温区窄，铝侧梯度小高温区范围广，冷却时高温区逐渐向钛侧偏移. 当钨极正对钛钝边时，等温线平行于钎焊界面，温度分布均匀，有利于形成组织均匀的界面反应层. 冷体熔钎焊加速了钎焊界面的冷却，降低了钛的溶解量，可抑制金属间化合物的生长. 化合物层形貌由空冷时的锯齿状转变为胞状生长.

关键词：Ti/Al 异种合金；熔钎焊；温度场
中图分类号：TG454　　**文献标识码**：A　　**文章编号**：0253－360X(2012)07－0013－04

吕世雄

0　序　　言

Ti/Al 复合构件既具有钛合金比强度高、低温韧性好和耐腐蚀的优势，又有铝合金的质轻、低成本等特点，可满足现代工业的轻量化、结构功能一体化和低成本设计与制造的要求[1]. 然而钛与铝物理化学性能差异显著，存在冶金学上的不相容性，焊接接头中易形成金属间化合物脆性相并产生应力集中，传统熔焊的方式难以实现二者的连接.

电弧熔钎焊是通过电弧将接头加热到两种材料熔点间的温度，低熔点母材熔化与液态焊丝形成熔焊连接，高熔点母材通过元素的溶解扩散与液态焊丝之间形成钎焊界面. 同时电弧具有阴极雾化去膜、电磁搅拌阻碍化合物生长、成本低和适应性强等优势，已成为异种材料连接的热门研究方法[2]. 为抑制 Ti/Al 界面反应进行，需严格控制钛的溶解量，以确保结合界面组织性能的均匀性[3]. 激光熔钎焊的研究发现接头厚度方向不均匀的热输入导致钎焊界面形成复杂的界面结构，反应层的厚度、形貌和物相差异巨大，致使熔钎焊的稳定性难以保证[4,5].

Ti/Al 熔钎焊接头焊缝两侧热物理性能差异显著，界面温度变化迅速，液态焊丝在两侧润湿铺展和熔合，使温度分布复杂化. 接头温度场对促进液态焊丝在钛侧的润湿铺展，改善接头组织分布以控制化合物的生长具有重要的意义. 通过有限元方法计算了 Ti/Al 电弧熔钎焊的温度场，研究了电弧加热位置对温度场分布的影响，分析了冷却方式对热循环与钎焊界面组织的变化规律，为优化熔钎焊工艺、改善焊缝成形和控制界面冶金反应提供依据.

1　有限元模拟计算

温度场数值模拟是将传热模型在时间和空间上离散化并建立离散化方程，再根据初始条件和边界条件结合材料参数求解离散方程，最终获得熔钎焊接头温度场的分布规律.

熔钎焊过程属于典型的热传输过程，温度分布满足基本的热传导微分方程. 接头温度取决于热源功率、测试点位置、冷却方式，同时受材料密度、热容和导热系数的影响. 热传导微分方程为

$$\frac{\partial T}{\partial t}=\frac{\lambda}{\rho c_{\mathrm{P}}}\left(\frac{\partial^2 T}{\partial x^2}+\frac{\partial^2 T}{\partial y^2}+\frac{\partial^2 T}{\partial z^2}\right)+\frac{Q}{\rho c_{\mathrm{P}}} \tag{1}$$

式中：T 为空间某点 t 时刻的温度；λ 为导热系数；ρ 为材料密度；c_{p} 为定压比热容；Q 为单位空间的热

收稿日期：2012－02－27
基金项目：国家自然科学基金资助项目(50974046 和 50904020)；哈尔滨市青年科技创新人才基金资助项目(2009RFQXG050)；中央高校基础科研业务费专项资金资助项目(HIT. NSRIF. 2012007)；国家博士后科学基金资助项目(20090460883；201003419)

功率.

通过 MARC 有限元软件计算 Ti/Al 熔钎焊接头的温度分布,几何模型为 100 mm × 40 mm × 2 mm 的 TC4 钛板与等尺寸的 LF6 铝板对接,采用八节点六面体单元进行网格划分. 为兼顾运算速度和精度,离焊缝较远的区域单元尺寸较大,以提高运算速度,焊缝附近采用较细的网格划分,以保证计算精度. 网格划分结果如图 1 所示.

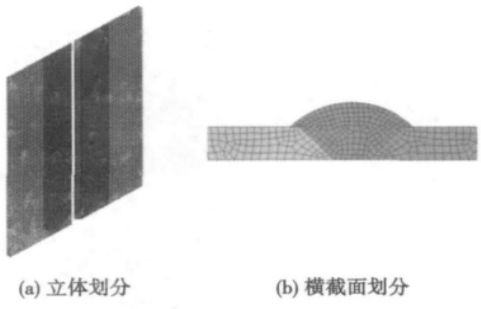

图 1 熔钎焊接头有限元网格划分

Fig. 1 Generated mesh of welding-brazed joint

采用分段线性化的方式考虑钛和铝热物理参数随温度的非线性变化. TC4 与 LF6 的密度分别为 4 450 kg/m^{3}和 2 640 kg/m^3,同时铝合金的相变潜热为 3.95×10^5 J/kg,熔化温度区间 580 ~ 625 ℃.

2 电弧熔钎焊试验

试验母材为 2 mm 厚的 TC4 钛合金和 LF6 铝合金,坡口角度为 90°,对接间隙 2 mm,背部加带成形槽的铜垫板. 选用 AlSi12 焊丝为填充材料,采用交流 TIG 电源进行熔钎焊试验. 成形槽内通入氩气以保证接头背部良好的润湿铺展,接头冷却包括空气冷却和水冷铜垫板(冷体)冷却两种方式.

通过 MARC 有限元分析软件模拟 Ti/Al 熔钎焊接头的温度场分布,考察了钛钝边的熔钎焊热循环特征,并通过扫描电镜观察该位置微观组织的结构特征.

3 结果与分析

3.1 Ti/Al 熔钎焊接头温度场特征

电弧功率为 2 000 W、焊接速度 120 mm/min 时,通过 MARC 有限元分析软件自动加载焊料填充过程,获得的 Ti/Al 熔钎焊接头正反面温度场分布如图 2 所示.

由图 2 可知,焊缝两侧温度场呈明显的非对称

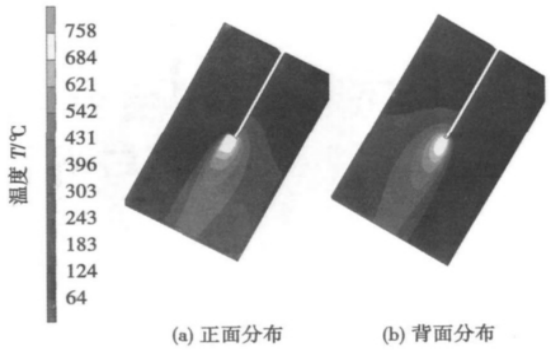

图 2 电弧熔钎焊温度场分布云图

Fig. 2 Temperature distribution of welding-brazed joint

分布,温度在钛合金侧分布集中,温度梯度大,而在铝合金侧高温区域较宽,温度梯度小. 由于 TC4 与 LF6 的导热系数差异显著,钛合金导热系数小,热流的传输受到阻碍,致使钛侧温度梯度大. 而铝合金导热系数大,热流容易传输到离焊缝较远的母材区域,形成较大范围的高温分布. 钛合金在温度超过 400 ℃时易发生氧化,焊接过程中需要对高温区域进行氩气保护,正反面温度场分布云图对正面氩气托罩和反面铜垫板设计有重要意义.

电弧熔钎焊属于局部热源加热,其温度场具有准稳态特征,分析不同位置截面的温度分布来模拟同一截面温度场随时间的变化,等距截面的温度分布如图 3 所示.

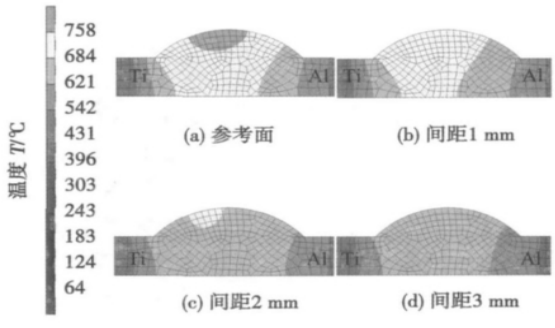

图 3 熔钎焊接头横截面温度场分布云图

Fig. 3 Temperature distribution at cross-sections of joints

由图 3 可知,钛合金与铝合金熔钎焊的冷却过程中,接头高温区逐渐向钛合金侧焊缝内聚集,从而延长了钎焊界面的高温停留时间. 促进了 Ti,Al 原子之间的相互扩散,为界面冶金反应提供了所需的动力学条件. 另外,铝合金侧冷却速度明显大于钛合金侧,有利于促进焊缝内金属间化合物的形核,促

使其在焊缝内弥散分布.

3.2　电弧加热位置对接头温度场的影响

电弧加热位置对温度场的分布起决定性的作用,加热位置主要包括焊枪钨极位置与电弧长度,综合考虑填丝与电弧的稳定性,电弧长度需控制在 4 ~6 mm. 通过调整 MARC 有限元模型焊接路径的加载节点位置,模拟钨极相对坡口的位置变化. 设坡口中心的偏移量为零,偏铝侧为正,偏钛侧为负,计算得到的不同偏移量下熔钎焊接头横截面的温度场如图 4 所示.

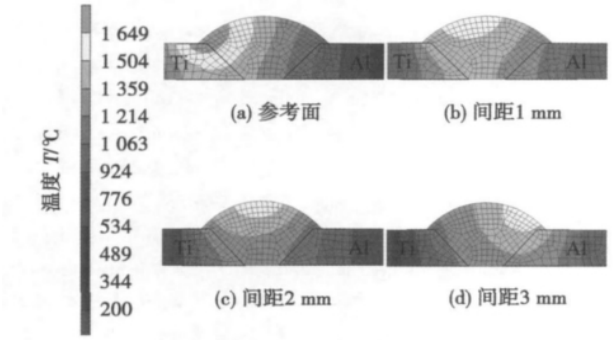

图 4　不同钨极偏移量下接头横截面温度分布云图

Fig. 4　Temperature distribution of joints with different offset

由图 4 可知,不同钨极偏移条件的 Ti/Al 熔钎焊接头的高温区均指向钛合金侧,与上述的接头高温区在钛侧聚集结果一致. 不同偏移量时熔钎焊接头横截面的温度分布变化显著. 当钨极偏向钛侧 2 mm 时,钛合金坡口顶部位置出现了过热现象,温度超过了钛合金的熔点. 实际熔钎焊坡口顶部的部分钛合金将发生熔化,熔化的钛与铝结合形成了大量的 Ti-Al 系金属间化合物,并在焊接应力作用下发生开裂,容易导致接头界面连接失效. 钨极居中(偏移量为零) 时,钛合金焊缝金属内存在明显的温度梯度,钛侧钎焊界面上温度分布较一致,但厚度方向上坡口底部高温区范围明显超过坡口顶部. 由此说明,钎焊界面底部冶金反应时间将长于顶部的冶金反应,从而容易形成较厚的界面反应脆性层. 当钨极偏向铝侧 2 mm 时,钛合金侧钎焊界面与等温线相交,也就是说钎焊界面上存在温度梯度,底部与顶部峰值温度相差约为 50 ℃以上. 峰值温度的差异可能导致界面冶金反应的过程改变,从而形成界面组织和性能的不均匀性.

当钨极偏钛侧 1 mm 时钎焊界面近乎平行于温度场的等温线,焊缝内部温度梯度不明显,如图 4b 所示. 均匀的温度场分布可形成厚度、形貌和物相一致的化合物反应层,有利于形成组织性能均匀的钎焊界面,同时也是促进液态焊丝在钛合金侧润湿铺展和改善熔钎焊接头成形的关键.

3.3　冷却方式对接头热循环的影响

Ti/Al 熔钎焊接头钎焊界面的形成本质是固态钛合金与液态焊丝之间化学元素的相互溶解和扩散的过程. 一方面,在化学势梯度的驱动下界面 Ti,Al 原子相互结合,从而降低体系的吉布斯自由能; 另一方面,由于 Ti-Al 系金属间化合物的生成,界面溶解动力学特征主要受接触表面层溶解的控制. 吉布斯自由能和溶解速度常数是界面冶金反应热力学与动力学的两大基本参数,二者均随温度变化而显著变化,因此合适的温度分布和热循环是形成优质 Ti/Al 钎焊界面的关键.

通过热电偶测温的方式测量钛侧钎焊界面的热循环过程,当焊接电流为 80 A,焊接速度为 120 mm/min 时,钛钝边处的热循环曲线如图 5a 所示. 对比发现热循环的计算值与试验值变化规律吻合良好,峰值温度相差在 50 ℃以内,冷却阶段二者相差明显,原因在于有限元模型的散热条件只考虑了工件的对流散热,实际散热过程还包括卡具的热传导和辐射散热过程.

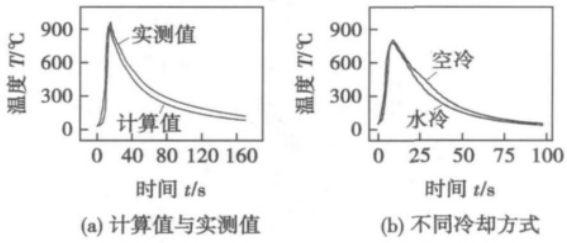

图 5　Ti/Al 钎焊界面热循环过程

Fig. 5　Thermal cycle of Ti-Al brazing interface

通过改变有限元模型中的对流换热系数来模拟冷却条件的变化,当电弧功率为 2 000 W,焊接速度为 180 mm/min 时,计算得界面中心在两种冷却条件下的热循环曲线如图 5b 所示.

由图 5b 可知,加热阶段空冷与冷体焊接的热循环温升速率、峰值温度相差不明显,而在冷却过程中冷体焊接时钎焊界面的高温停留时间明显缩短,冷却速度加快,将直接影响 Ti/Al 熔钎焊接头中钎焊界面的化合物层的形核与长大.

3.4　冷却方式对界面微观组织的影响

基于以上的有限元分析与焊缝成形,实际熔钎焊时需将钨极位置确定为钛侧钝边偏焊缝 0.5 mm 位置. 在不同热输入与冷却方式下进行熔钎焊正交试验,焊后对熔钎焊接头横截面取样,制备金相试样

并观察钎焊界面的组织特征,结果如图 6 所示.

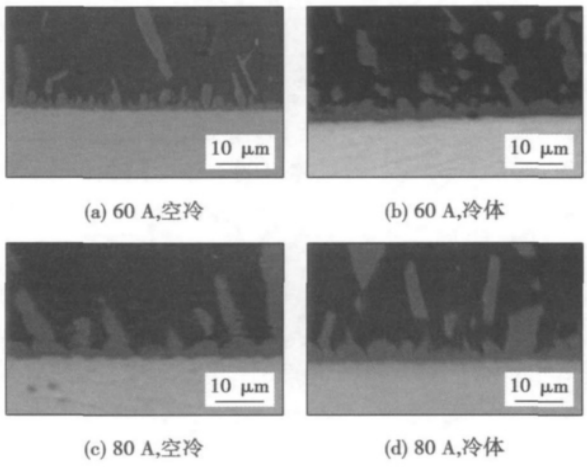

图 6 Ti/Al 电弧熔钎焊接头界面组织

Fig. 6 Interfacial microstructure of welding-brazed joints

区别于化合物在 Ti/Al 扩散焊接头中的连续层状分布[6,7],电弧熔钎焊界面呈择优取向竞争生长,其厚度小于 10 μm. 激光熔钎焊试验研究也发现 Y 形坡口钝边位置极易形成冶金反应不良[8],TIG 焊电弧加热可避免坡口钝边的冶金反应不足. 空气冷却时金属间化合物呈锯齿状生长,局部位置甚至呈柱状生长,冷体条件下金属间化合物的“锯齿”长度明显减小,当焊接电流 $I_w = 60$ A 时金属间化合物呈胞状分布. 当 $I_w = 80$ A 时,相对于低电流界面特征金属间化合物明显长大,另外两种冷却方式下的界面反应层形貌和厚度相差较小,说明冷体条件对控制金属间化合物生长的效果相对较弱. 因此在 Ti/Al电弧熔钎焊的过程中需从热输入和冷却条件两方面来控制钎焊界面金属间化合物的生长,较低的热输入与冷体焊接可形成较理想的界面组织结构.

4 结 论

(1) Ti/Al 熔钎焊接头温度场呈非对称分布,钛侧梯度大高温区窄,铝侧梯度小高温区范围广. 冷却时高温区逐渐向钛侧偏移.

(2) 钨极位置决定了接头温度场的分布特征,正对钛钝边时等温线平行于钎焊界面,焊缝内温度分布均匀,改善了界面温度的非均匀性.

(3) 冷体熔钎焊时冷却速度增加高温停留时间缩短,可降低钛合金母材的溶解量. 冷体焊接可抑制金属间化合物的生长,促使其呈胞状分布.

参考文献:

[1] Möller F, Grden M, Thomy C, *et al*. Combined laser beam welding and brazing process for aluminium titanium hybrid structures [J]. Physics Procedia, 2011, 12(A): 215 – 223.

[2] Song Jianling, Lin Sanbao, Yang Chunli, *et al*. Spreading behavior and microstructure characteristics of dissimilar metals TIG welding-brazing of aluminum alloy to stainless steel [J]. Materials Science and Engineering A, 2009, 509(1/2): 31 – 40.

[3] Lü Shixiong, Xu Zhiwu, Wang Haitao, *et al*. Investigation on TIG cladding of copper alloy on steel plate [J]. Science and Technology of Welding and Joining, 2008, 3(1): 10 – 16.

[4] Chen Yanbin, Chen Shuhai, Li Liqun, *et al*. Effects of heat input on microstructure and mechanical property of Al/Ti joints by rectangular spot laser welding-brazing method [J]. International Journal of Advanced Manufacturing Technology, 2009, 44(3 – 4): 265 – 272.

[5] 封小松, 陈树海, 李俐群, 等. 铝钛异种合金激光熔钎焊接头温度分布 [J]. 焊接学报, 2009, 30(10): 9 – 16.
Feng Xiaosong, Chen Shuhai, Li Liqun, *et al*. Temperature distribution of Al/Ti dissimilar alloys joint in laser welding brazing [J]. Transactions of the China Welding Institution, 2009, 30(10): 9 – 16.

[6] AlHazaa A, Khan T I, Haq I. Transient liquid phase (TLP) bonding of Al7075 to Ti-6Al-4V alloy [J]. Materials Characterization, 2010, 61(3): 312 – 317.

[7] Sohn W H, Bong H H, Song H. Microstructure and bonding mechanism of Al/Ti bonded joint using Al-10Si-1Mg filler metal [J]. Materials Science Engineer A, 2003, 355(1 – 2): 231 – 240.

[8] 陈树海, 李俐群, 陈彦宾. 光斑形式对 Ti/Al 异种合金激光熔钎焊特性的影响 [J]. 焊接学报, 2008, 29(6): 49 – 52.
Chen Shuhai, Li Liqun, Chen Yanbin. Welding characteristics of Al/Ti dissimilar alloys by laser welding-brazing with different spot [J]. Transactions of the China Welding Institution, 2008, 29(6): 49 – 52.

作者简介: 吕世雄,男,1957 年出生,博士,教授级高级工程师. 主要从事有色金属焊接与特种焊接方面的科研工作. 发表论文 20 余篇. Email: lvshixiong_hit@163.com

通讯作者: 黄永宪,男,讲师. Email: yxhuang@hit.edu.cn

MAIN TOPICS, ABSTRACTS & KEY WORDS

Microstructure and stress-rupture property of TLP diffusion bonded DD3 single crystal superalloy joints LI Xiaohong[1], MAO Wei[1], ZHONG Qunpeng[2], CAO Chunxiao[1], XIONG Huaping[1] (1. Lab of Welding and Forging, Beijing Institute of Aeronautical Materials, Beijing 100095, China; 2. School of Material Science and Engineering, Beihang University, Beijing 100191, China). pp 1 - 4

Abstract: DD3 is a first generation nickel-based single crystal superalloy developed in China. In order to meet the possible need of manufacturing turbine blades and vanes, DD3 was TLP diffusion bonded with D1P powder interlayer alloy and the investigation on joint microstructure and properties was conducted. The results showed that, the bonding seam was mainly composed of $\gamma+\gamma'$ two-phase matrix, dendritic compound was identified as $(Mo,W,Cr,Ni)_3B_2$ and strip-like compound was identified as $(Cr,Mo)_{23}(C,B)_6$. Some blocky or needle-like compounds were precipitated in the zone adjacent to the bonding seam, and the TEM analysis results indicated that these compounds were identified as $(Mo,W,Cr,Ni)_3B_2$ borides. Microstructural inhomogeneity existed in the joint along the flowing direction of molten interlayer alloy, and this inhomogeneity could not be eliminated even by the diffusion bonding for 24 h at elevated-temperature of 1 250 ℃. There are some γ' phases in the form of large block. The boundaries between these large γ' phases and the bonding seam matrix became the weak part of the joint, which damaged the joint property. Under proper bonding condition, the stress-rupture strength at 980 ℃ of the TLP diffusion bonded DD3 alloy joints reached 90% of that of the base metal.

Key words: single crystal superalloy; TLP diffusion bonding; joint microstructure; joint stress-rupture property

Finite element analysis of magnetic control arc welding seam tracking sensors HONG Bo, LI Lin, HONG Yuxiang, YANG Jiawang (School of Mechanical Engineering, Xiangtan University, Xiangtan 411105, China). pp 5 - 8

Abstract: In order to research the electromagnetic characteristics of the magnetic control arc welding seam tracking sensors, the harmonic magnetic field of sensor is analyzed with ANSYS software: when the coil circle number, air gap length, core magnetic conductance factors change respectively, the magnetic control arc welding seam tracking sensors magnetic maps and magnetic field vector diagram are obtained. The influence law of the main parameters of arc sensor on the magnetic field distribution and the size of the magnetic induction is analyzed, and is compared with the actual magnetic induction intensity measured by gauss plan. The results show that analysis results of using the finite element method for magnetic control arc sensor electromagnetic properties and test results are coincide. It provides theoretical guidance for magnetic control arc welding seam tracking technology.

Key words: magnetic control arc; seam tracking; sensor; finite element analysis

Laser-tandem MIG hybrid welding for 6005A-T6 aluminum alloy profile of high-speed train WANG Xuyou[1], LEI Zhen[1], ZHANG Jian[1], WANG Yanjin[2] (1. Harbin Welding Institute, China Academy of Machinery Science & Technology, Harbin 150080, China; 2. Changchun Railway Vehicles Co., Ltd., Changchun 130062, China). pp 9 - 12

Abstract: Welding research of 6005A-T6 aluminum alloy profile for high-speed train was done by using tandem MIG welding and laser-tandem MIG hybrid welding individually. The weld appearance, welding distortion, mechanical properties of the joints and microstructure were analyzed. The results demonstrated that high-efficient welding for the profile was achieved by using laser-tandem MIG hybrid welding, the speed of which was up to 4.5 m/min. The process had a good gap bridging ability that even if the gap of the butt joint was up to 1.4 mm, a good weld appearance could also be got. While the hybrid welding speed was greater than 4 m/min, the welding distortion of the laser-tandem MIG hybrid joints was just about 40% of that of the tandem MIG joints. And tensile strength of the hybrid joints was 83% of that of 6005A-T6 base metal, 9% higher than that of the tandem MIG joints.

Key words: high-speed train; aluminum alloy profile; laser; tandem MIG arc; hybrid welding

Investigation on temperature field and interfacial microstructure of Ti/Al arc welding-brazing joint LÜ Shixiong[1], JING Xiaojun[1,2], HUANG Yongxian[1], WANG Yuanrong[2], LI Shufei[2], XU Yongqiang[1] (1. State Key Laboratory of Advanced Welding and Joining, Harbin Institute of Technology, Harbin 150001, China; 2. Chengdu SIWI High-Tech Industrialized Garden Co., Ltd, Chengdu 611731, China). pp 13 - 16

Abstract: Dissimilar alloys of TC4 titanium alloy and LF6 aluminum alloy were butt joined successfully by TIG arc and Al-Si12 filler metals. Temperature distribution and relationship were investigated by finite element method (FEM) numerical simulation and experimental validation. The microstructure of the interfacial layers was measured by scanning electron microscopy (SEM). The results indicate that the temperature distribution of Ti/Al arc welding-brazing joint is extremely asymmetrical, the titanium side exhibits high temperature gradient and narrow high-temperature zone, while the aluminum side exhibits low temperature gradient and wide high-temperature zone. The high-temperature zone trends to assemble near the titanium side in cooling stage. The interface roughly parallel to the isotherm of the temperature field as the electrode point at titanium root face. This leads to a symmetrical temperature distribution at brazing interface and seam near titanium side, which can improve interfacial reaction nonhomogeneity. It is the key factor to form brazing interface with symmetrical microstructure and welding-brazing joint with high performance. The water cooling technology can acceler-

ate the cooling process, cutting down the dissolution of titanium and retard the growth of intermetallic compounds. The interfacial reaction layer morphology is cellular rather than serrated shape in air cooling condition.

Key words: Ti/Al dissimilar alloy; welding-brazing; temperature field

Method of pulsed-MIG welding arc voltage control based on sub-spraying transfer LIN Fang[1], WEI Zhonghua[2], CHEN Xiaofeng[2], CUI Longbin[2], XUE Jiaxiang[2] (1. Department of Electromechanical Technology, Jiangmen Polytechnic, Jiangmen 529000, China; 2. School of Mechanical & Automotive Engineering, South China University of Technology, Guangzhou 510640, China). pp 17 - 20

Abstract: Constant current control and constant wire feed were both used in the pulsed metal argon arc welding power source. The method of pulsed-MIG welding arc voltage control based on sub-spraying transfer was put forward. Its principle is as follows: the average arc voltage of each period of pulse was measured. If the average arc voltage was within the sub-spraying transfer range, the arc length would be adjusted only by self-adjusting of the arc. But if the average arc voltage went beyond the sub-spraying transfer range, the background current time changed so that the average current in each pulse period changed, so did the burn-off rate in the welding conditions above. It was found that the arc adjustment and anti-disturbance ability were improved. The results of the tests indicated this method obviously improved the welding dynamic characteristics and efficiently restrained disturbances. In addition, well-formed welding seams were acquired.

Key words: pulsed metal argon arc welding; sub-spraying transfer; arc voltage control

Symmetrical transition waveform control process of double wire MIG welding YAO Ping[1], XUE Jiaxiang[2], Ma Qianjin[2], CHEN Hui[2], CHEN Xiaodong[2] (1. College of Electromechanical Engineering, Guangdong Polytechnic Normal University, Guangzhou 510635, China; 2. School of Mechanical and Automotive Engineering, South China University of Technology, Guangzhou 510640, China). pp 21 - 24

Abstract: In order to reduce the impact of electromagnetic force in double-wire welding and the probability of breaking arc during switching between peak current and basic current, a symmetrical transition waveform control process for double-wire MIG welding is proposed. The new process tries to improve symmetrical transition during the change of double-wire phase, and introduce three control parameters: leading-wire transition current I_{s1}, double-wire transition time T_s and trailing-wire transition current I_{s2}. Orthogonal experiment was designed and the results were analyzed and assessed by range analysis method. It shows that the impacts of I_{s1}, T_s and I_{s2} on welding quality decrease in turn. Further verification test shows that the range of operating point is wider, the welding process is more smooth and soft, and weld surface produces a glossy transition zone. This paper provides a new idea for waveform control of double-wire welding.

Key words: double wire MIG welding; symmetrical transition; waveform control; orthogonal experimental; range analysis

Analysis of mechanism for TIG-MIG hybrid arc properties YANG Tao[1], ZHANG Shenghu[1], GAO Hongming[1], WU Lin[1], XU Kewang[2], LIU Yongzhen[2] (1. State Key Laboratory of Advanced Welding and Joining, Harbin Institute of Technology, Harbin 150001, China; 2. Offshore Oil Engineering Co. Ltd, Tianjin 300451, China). pp 25 - 28, 60

Abstract: TIG-MIG hybrid arc is adopted to change deficiencies existing in TIG or MIG welding method. With PID theory, current and voltage of welding power is constantly controlled to achieve TIG and MIG hybrid arc. Thus, property of hybrid arc, transitional form of droplet and influence of different polarity connections to welding seam are studied. Results from above research show that presence of TIG arc made good effect for stability of MIG arc. In the hybrid welding, following minimum voltage rule, TIG arc burns on droplet to heat metal and DCEP has good effect in cleaning oxide film of workpiece. In conclusion, TIG-MIG hybrid arc efficiently reduce welding splash, promote wetting of droplets and formation of welding seam, and realize welding with higher efficiency and better quality.

Key words: hybrid arc; droplet transfer; weld formation; high-efficiency welding

Research on ultrasonic metal welding power supply based on DSP YANG Jingwei, CAO Biao, YIN Tiangang (School of Mechanical & Automotive Engineering, South China University of Technology, Guangzhou 510640, China). pp 29 - 32

Abstract: The analog power supply of ultrasonic welding has the shortages of inaccurate frequency tracking and unadjustable amplitude in the process of welding, which make the welding process unstable, sometimes even lead to failure. The design scheme based on digital signal processor (DSP) was proposed to improve the reliability and stability of ultrasonic metal welding. Frequency tracking was realized by using incremental PI algorithm through gathering phase difference signal between voltage and current of piezoelectric transducer (PZT). The method of pulse width modulate (PWM) was used to control and adjust the amplitude of ultrasonic vibration. The results indicated the ultrasonic welding power supply based on DSP could adjust the amplitude continuously and track the resonant frequency in 0.32 ms during the welding process.

Key words: ultrasonic welding power supply; frequency tracking; piezoelectric transducer; incremental PI algorithm

Effect of Cu + B composite fillers proportion on Al_2O_3/TC4 alloy joint microstructure YANG Minxuan[1], LIN Tiesong[1,2], HAN Chun[1], HE Peng[1], WEI Hongmei[1] (1. State Key Laboratory of Advanced Welding and Joining, Harbin Institute of Technology, Harbin 150001, China; 2. Department of Electronics Packaging Technology, School of Materials Science and Engineering, Harbin Institute of Technology, Harbin 150001, China). pp 33 - 36, 40

Abstract: The composite fillers with different proportions of Cu and B powders were used to braze Al_2O_3 to TC4 alloy at 930 ℃ for 10 min. The joining and microstructure of Al_2O_3/TC4 alloy joints were observed and analyzed by SEM and EDS. The results show that Al_2O_3/TC4 alloy joint interfacial microstructure is Al_2O_3/Ti_3(Cu, Al)$_3O$/Ti_2Cu + Ti_2(Cu, Al)/Ti + Ti_2(Cu, Al) + Ti(Cu, Al) + $AlCu_2Ti$ + Ti_2Cu/Ti_2Cu + $AlCu_2Ti$ + TiB/Ti